AIP Applied Physics Letters

Calculation of temperature dependent threshold current density of ZnCdSe/ZnSe quantum well laser including many body effects

A. Bandyopadhyay and P. K. Basu

Citation: Appl. Phys. Lett. 70, 553 (1997); doi: 10.1063/1.118336
View online: http://dx.doi.org/10.1063/1.118336
View Table of Contents: http://apl.aip.org/resource/1/APPLAB/v70/i5
Published by the American Institute of Physics.

Calculation of temperature dependent threshold current density of ZnCdSe/ZnSe quantum well laser including many body effects

A. Bandyopadhyay[a)]
Central Electronics Engineering Research Institute, Pilani 333 031, India

P. K. Basu
Institute of Radio Physics & Electronics, University of Calcutta, Calcutta 700 009, India

(Received 7 April 1996; accepted for publication 28 November 1996)

We have calculated the threshold current density of the ZnCdSe/ZnSe quantum well laser as a function of temperature by incorporating many body Coulomb interactions, both the heavy- and light hole subbands, as well as the temperature and energy dependencies of linewidth for laser transition. The effect of finite well width and well depth in the Coulomb interaction is also considered instead of taking strictly two-dimensional Coulomb potential. The calculated values of nominal threshold current density are 1.5 times larger than the values calculated without considering Coulomb interaction, whereas calculations using strictly two-dimensional Coulomb potential show 7% overestimation. Good agreement is obtained between the reported experimental results and the theoretical threshold current densities for a $Zn_{0.83}Cd_{0.17}Se/ZnSe$ multiple quantum well laser assuming a value of 0.8 for the internal quantum efficiency. © *1997 American Institute of Physics.* [S0003-6951(97)03605-X]

Recently there has been a widespread interest in II–VI semiconductor lasers emitting in the blue green region of the visible spectrum. Lasing action in II–VI semiconductor quantum wells (QWs) has been demonstrated up to room temperature in several laboratories.[1,2] However the optical gain mechanism in II–VI material systems, especially at and around room temperature, is still uncertain. Ding *et al.*[3] have claimed that the optical gain in ZnCdSe/ZnSe quantum-well lasers is of excitonic nature at least up to a temperature of 220 K. In an alternative approach, the electron–hole interaction has been incorporated into the calculation of optical gain in II–VI bulk as well as QW materials and the effect is found to be significant.[4–6] The gain spectra of II–VI QW lasers have been calculated by deriving an expression for optical susceptibility from the screened Hartree–Fock approximation to full many body problems.[5,6] In this letter we use a similar formalism to incorporate many body Coulomb effects in the calculation of nominal threshold current density (J_{thn}) of $Zn_{0.83}Cd_{0.17}Se/ZnSe$ quantum well lasers at different temperatures. We consider both heavy- and light-hole subbands in calculating absorption and spontaneous recombination rates. The linewidths for electron–heavy hole and electron–light hole transitions are calculated as a function of wave vector (**k**) at different temperatures considering carrier and carrier-LO phonon scattering mechanisms. Furthermore, instead of taking the strictly two dimensional (2D) Coulomb potential, the finite well width and well depth are taken into account in our calculation. We have found that the 2D Coulomb potential overestimates the electron-hole effect and leads to a slightly higher value of J_{th}. In order to estimate the threshold current density as a function of temperature the leakage current density at threshold is calculated using both the drift and diffusion contributions in the n- and p- cladding layers. Our calculated values of the threshold current density as a function of temperature for a $Zn_{0.83}Cd_{0.17}Se/ZnSe$ multiple quantum well (well width: 60 Å; number of wells: 6) laser are then compared with the reported experimental results[7] taking the internal quantum efficiency as a fitting parameter, and good agreement with experimental results is obtained for an internal quantum efficiency of 0.8. It is found that the linewidths for both electron–heavy hole and electron–light hole transitions increase by a factor of 1.5 as the temperature increases from 200 K to room temperature. This effect is important in correctly predicting the variation of J_{thn} with temperature.

The complex susceptibility $\chi\,(\omega,n)$ at frequency ω and injected carrier density n is related to microscopic polarization $\chi^{\alpha\beta}\,(\mathbf{k},\omega)$ as[8]

$$\chi(\omega,n)=\sum_{\mathbf{k}}\mu^{\alpha\beta}(\mathbf{k})\chi^{\alpha\beta}(\mathbf{k},\omega)/\Omega, \tag{1}$$

where $\mu^{\alpha\beta}\,(\mathbf{k})$ is the dipole matrix element between the αth conduction and the βth valence subbands at a wavevector **k**, Ω is the volume of the QW. $\chi^{\alpha\beta}\,(\mathbf{k},\omega)$ obeys the relation

$$\chi^{\alpha\beta}(\mathbf{k},\omega)=-\mu^{\alpha\beta}(\mathbf{k})\frac{1-f^{\alpha}_{e\mathbf{k}}-f^{\beta}_{h\mathbf{k}}}{[\hbar\omega-E^{\alpha\beta}(\mathbf{k})]+i\Gamma^{\alpha\beta}}\times\left(1+\frac{1}{\mu^{\alpha\beta}(\mathbf{k})}\sum_{\mathbf{k}'}V^{\alpha\beta}_{s}(|\mathbf{k}-\mathbf{k}'|)\chi^{\alpha\beta}(\mathbf{k}',\omega)\right), \tag{2}$$

where $f_{i\mathbf{k}}(i=e,h)$ is the quasi-Fermi function, $E^{\alpha\beta}(\mathbf{k})$ is the energy difference between αth conduction and βth valence subbands at wave vector **k** including band gap renormalization,[8] and $\Gamma^{\alpha\beta}$ is the corresponding transition linewidth. The Fourier transform of screened Coulomb potential is given by $V^{\alpha\beta}_{s}(\mathbf{q})/\epsilon_{s}(\mathbf{q},\omega)$, where $\epsilon_{s}(\mathbf{q},\omega)$ is the permittivity calculated in statical single plasmon pole approximation.[8] The unscreened Coulomb potential $V^{\alpha\beta}(\mathbf{q})$

[a)]Present address: School of Engineering Science, Simon Fraser University, Burnaby, British Columbia V5A 1S6, Canada. Electronic mail: anirban@sfu.cs.ca between an electron in αth subband and a hole in βth subband has been calculated by expressing the wave function of electron (hole) $\phi_{\alpha(\beta)}(z_{\alpha(\beta)})$

$$V^{\alpha\beta}(\mathbf{q})=V_{2d}(\mathbf{q})\int\int \epsilon_w\epsilon^{-1}(z_\alpha,z_\beta)|\phi_\alpha(z_\beta)|^2 \times\exp(-q|z_\alpha-z_\beta|)dz_\alpha dz_\beta. \quad (3)$$

As the well width $d\rightarrow 0$ and the well depth $\rightarrow\propto$, $V^{\alpha\beta}(\mathbf{q})$ reduces to the expression for the two-dimensional Coulomb potential $V_{2d}(\mathbf{q})=e^2/(2qA\epsilon_w)$, where ϵ_w is the permittivity inside the well and A is the area of the QW. The quantity $\epsilon(z_\alpha,z_\beta)$ is equal to ϵ_w when z_α and z_β are within the well, is equal to ϵ_b (pemittivity of the barrier) when z_α and z_β are outside the well, and becomes the average of ϵ_w and ϵ_b in all other cases. In calculating $\epsilon_s(q,\omega)$ multisubband formalism[10] with two electron, two heavy-hole, and one light-hole subbands is used. The absorption coefficient (gain) $\alpha(\omega)$ is obtained from the imaginary part of the susceptibility.

In order to calculate the spontaneous recombination rate per unit volume (R_{sp}) from the above formalism we first determine the stimulated emission $g(\omega)$ from Eq. (2) replacing the band-filling factor $(1-f_{e\mathbf{k}}-f_{h\mathbf{k}})$ by $f_{e\mathbf{k}}f_{h\mathbf{k}}$ and proceeding similarly as for $g(\omega)$. R_{sp} is then calculated by using the following relation:

$$R_{sp}=\frac{N_w}{L^3}\sum_{\mathbf{p},\lambda}\frac{c}{\bar{n}}g(\omega_{\mathbf{p},\lambda}). \quad (4)$$

In Eq. (4) L^3denotes the reference volume, N_w is number of wells, $\mathbf{p}$ and λ label, respectively, the photon wave vector and polarization, c is the velocity of light, and $\bar{n}$ is the refractive index of the material.

The material parameters used in our calculations are taken from Ref. 11. Considering the biaxial compressive strain in the ZnCdSe layers, we calculate the strain induced shift in heavy–hole and light–hole bands and the effective masses parallel and perpendicular to the well plane.[11] The transition linewidth $\Gamma^{\alpha\beta}$ in Eq. (2) is calculated as a function of wave vector at different temperatures from the lifetimes due to carrier–carrier and carrier–LO phonon scattering mechanisms. Details of the calculation are given in Ref. 12.

By evaluating the total spontaneous recombination rate per unit volume for injected carrier density at threshold (n_{th}), we calculate the nominal threshold current density J_{thn} from the relation $J_{thn}=edR_{sp}$, where e is the electronic charge and d is the QW width. The threshold current density J_{th} is calculated from $J_{th}=J_{thn}/\eta+J_p+J_n$, where η is the internal quantum efficiency and J_p and J_n are, respectively, the leakage current densities in p and n cladding layers at threshold. The values of J_p and J_n are calculated using the expression given in Ref. 11 which incorporates both drift and diffusion contributions.

Figure 1 shows the absorption spectra for a multiquantum well (MQW) $Zn_{0.83}Cd_{0.17}Se/ZnSe$ laser calculated with and without Coulomb interaction with $N_w=6$, $d=60$ Å, barrier width of 100 Å, and an injected carrier density of 3.4×10^{18} cm^{-3}. The absorption spectra calculated using two-dimensional Coulomb potential is also shown in the figure. The neglect of Coulomb interaction results in reduction

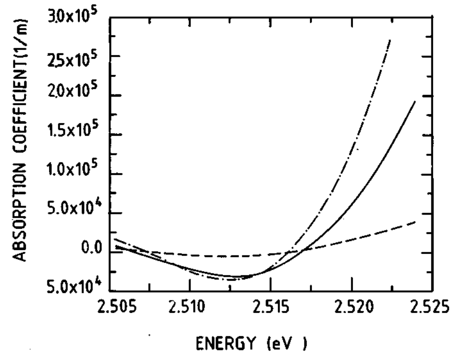

FIG. 1. Calculated absorption spectra for a MQW $Zn_{0.83}Cd_{0.17}Se/ZnSe$ laser with $N_w=6$, $d=60$ Å, and barrier width of 100 Å considering finite well width and well depth (solid curve), purely 2D Coulomb potential (dash-dotted curve) and without Coulomb interaction (dashed curve) at a carrier density of 3.4×10^{18} cm^{-3} at 300 K.

of absorption as well as maximum gain. For the QW structure considered, the maximum gain decreases by 300 cm^{-1} from the value obtained using Coulomb potential with finite well depth and well width. The 2D Coulomb potential overestimates the real electron–hole potential which leads to slightly higher gain at a given carrier density and steeper rise from the gain to absorption at higher energy.

We have considered in this work two electron and two heavy–hole subbands and one light–hole subband. The intraband scattering rates for the above QW are calculated at different carrier concentrations and at different temperatures as a function of wave vector ($\mathbf{k}$) for first electron ($1e$), heavy–hole (1hh) and light–hole (1lh) subbands. The average of total carrier and LO-phonon broadenings for electrons and heavy (light) holes is used to obtain the linewidth. The linewidth of $2e$–2hh transition is taken to be the same as that of the $1e$–1hh transition. Although this assumption underestimates the linewidth of $2e$–2hh transition, it does not affect the calculation of threshold carrier density significantly as an energy of $2e$–2hh transition is far off from the energy at maximum gain. The reduction of total broadening (carrier–carrier and carrier–phonon) is less than 10% at the highest wave vector considered in the calculations (corresponds to an energy of $\sim 10kT$) from the value at the band edge for all the subbands. Figure 2 shows the linewidth at electron–heavy

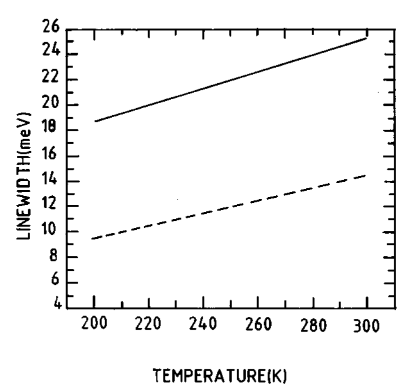

FIG. 2. Calculated linewidth as a function of temperature used in the calculation of J_{th} for first electron–heavy hole (solid) and first electron–light hole subband (dashed). The carrier density at each point is the threshold carrier density at that temperature.

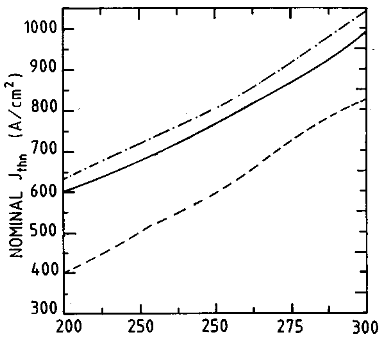

FIG. 3. Nominal threshold current density as a function of temperature. The solid line indicates calculation considering finite well width and well depth; the dash-dotted line is for calculation with 2D Coulomb potential and dashed line for calculation without Coulomb interaction.

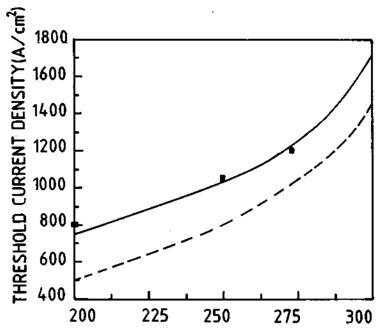

FIG. 4. Threshold current density as a function of temperature. The square dots are experimental data reported in Ref. 7. The solid line represents calculation considering finite well width and well depth; the dashed line is for calculation without Coulomb interaction.

hole (e–hh) and electron–light hole (e–1h) band edges as a function of temperature. The carrier concentration considered at each temperature is the threshold carrier concentration (n_{th}). Linewidth and n_{th} are calculated iteratively at each temperature using Eq. (2), threshold gain g_{th} required to overcome cavity loss, and the relations for carrier–carrier and carrier–LO phonon scattering lifetime given in Ref. 12. Our calculation shows that the broadening of electron–heavy hole transition is almost twice that of electron–light hole transition. This follows from the mass difference of the heavy and light holes. The overall linewidth for both e–hh and e–1h transitions increases by a factor of 1.5 between 200 K and room temperature. Our calculated value of e–hh linewidth at room temperature (25.34 meV in Fig. 2 corresponding to a lifetime of 26 fs) compares favorably with one considered in Ref. 13 to fit experimental data for a 65 Å ZnSe QW.

The calculated values of J_{thn} as a function of temperature are shown in Fig. 3. J_{thn} calculated without Coulomb effect is 1.5 times less than the values obtained using Coulomb potential with finite well width and well depth while the calculation with 2-D Coulomb potential overestimates J_{thn} by 7%. We consider a cavity length of 1 mm and scattering loss of 350 m^{-1} as considered in Ref. 7. Our calculated values of facet reflectance ($|r|^2$) and confinement factor (Γ) are 0.224 and 0.058, respectively. These lead to a threshold gain of 31 680 m^{-1}. To estimate total threshold current density J_{th}, values of J_p and J_n are needed. Since the thickness of cladding layers are not mentioned in the structure given in Ref. 7, we have taken a standard value of 1.5 μm. However, we find that J_p and J_n are not very sensitive to respective cladding layer thickness. The total leakage current density varies from 3.5 A/cm^2 at 200 K to 283 A/cm^2 at room temperature. Since internal quantum efficiency η is not known, we take it as a parameter and find J_{th} as a function of temperature for different η. Figure 4 shows the experimental values of J_{th} as reported in Ref. 7 along with the best-fitted calculated values obtained for η=0.8. Calculations performed without Coulomb effect give 1.5 times lower values for the above η.

In conclusion, we have calculated the temperature variation of the threshold current density for the ZnCdSe/ZnSe QW laser using many body Coulomb interaction taking into account finite well width and well depth, both heavy- and light-hole subbands and wave vector dependent carrier–carrier and carrier–LO phonon scattering lifetimes. We have shown that for a $Zn_{0.83}Cd_{0.17}Se$/ZnSe multiple quantum well of 60 Å well width neglect of Coulomb interaction leads to 1.5 times less threshold current density. The calculation with strictly 2-D Coulomb potential overestimates threshold current density by 7%.

[1] A. V. Nurmikko and R. L. Gunshor, IEEE J. Quantum Electron. **30**, 619 (1994).
[2] N. Nakayama, S. Itoh, T. Ohata, K. Nakano, H. Okuyama, M. Ozawa, A. Ishibashi, M. Ikeda, and Y. Mori, Electron. Lett. **29**, 2194 (1993).
[3] J. Ding, M. Hagerott, T. Ishihara, H. Jeon, and A. V. Nurmikko, Phys. Rev. B **47**, 10 528 (1993).
[4] J. Z. Zheng, Electron. Lett. **30**, 224 (1994).
[5] W. W. Chow and S. W. Koch, Appl. Phys. Lett. **66**, 3004 (1995).
[6] P. Rees, F. P. Logue, J. F. Donegan, J. F. Heffeman, C. Jordan, and J. Hegarty, Appl. Phys. Lett. **67**, 3780 (1995).
[7] R. L. Aggarwal, J. J. Zayhowski, and B. Lax, Appl. Phys. Lett. **62**, 2899 (1993).
[8] H. Haug and S. W. Koch, *Quantum Theory of the Optical and Electronic Properties of Semiconductors*, 2nd ed. (World Scientific, Singapore, 1993).
[9] G. P. Bava and P. Debernardi, Electron. Lett. **27**, 603 (1991).
[10] D. Campi, P. Bradley, R. Calvani, and R. Caponi, IEEE J. Quantum Electron. **29**, 1144 (1993).
[11] Y-h. Wu, IEEE J. Quantum Electron. **30**, 1562 (1994).
[12] M. Asada, IEEE J. Quantum Electron. **25**, 2019 (1989).
[13] P. M. Mensz, Appl. Phys. Lett. **65**, 2627 (1994).